Hindawi
Shock and Vibration
Volume 2020, Article ID 1452159, 9 pages
https://doi.org/10.1155/2020/1452159

Research Article

Dynamic Behavior and Fatigue Damage Evolution of Sandstone under Uniaxial Cyclic Loading

Yidan Sun, Yu Yang, and Min Li

School of Civil Engineering, Liaoning Technical University, Fuxin 123000, China

Correspondence should be addressed to Yu Yang; yangyu9300@163.com

Received 24 October 2019; Accepted 28 March 2020; Published 16 April 2020

Academic Editor: Cristina Castejón

The mechanical response characteristics of sandstone specimens under different stress amplitudes and loading frequencies were tested by a TAW-2000 rock triaxial testing machine. The characteristics of the stress-strain curve and the evolution process of strain damage under cyclic loading are analyzed. Based on creep theory and the disturbance state concept, a theoretical model between the axial compressive strain, axial compressive stress, and cycle number is established. The results show that there exists an upper threshold value of stress in cyclic loading above which the specimen will be damaged. As peak stress increases, the energy loss and irreversible deformation caused by damage gradually increase. When loading to an unstable peak stress under cyclic loading, the fatigue damage of sandstone under cyclic loading undergoes three characteristic stages: the initial stage; the stable stage; and the accelerated failure stage. The parameters of the strain damage model based on the disturbance state concept of sandstone are identified by test data, and the rationality of the model is validated by comparing theoretical values with experimental measurements.

1. Introduction

In addition to static loads, the surrounding rock near roadways will also be disturbed by dynamic loads such as drilling, mechanical excavation, or earthquakes from mining processes [1]. The mechanical properties of rock under cyclic loads are very different from those under static loads, and its mechanical behavior is more complex [2, 3]. Therefore, it is of great significance to study the dynamic behavior and fatigue damage evolution laws of rock subjected to cyclic loading in order to assess the stability of rock formations surrounding roadways.

Laboratory testing is the primary method used to understand rock mechanical behavior. In previous decades, scholars have little researched rock mechanical responses under cyclic loading. There are some studies on the dynamic response characteristics of various types of rock under coupled static-dynamic loading and high-stress conditions [4–7], and the results have revealed the mechanism of deep rock burst. Song et al. [8] carried out cyclic loading tests on salt rock samples and determined the fatigue life of rock salt samples under different upper and lower stresses, cyclic loading speeds, temperatures, and confining pressures. Fan [9] further quantified the fatigue life and deformation evolution characteristics of salt rock by subjecting it to different stress amplitudes. Wang et al. [10] established the constitutive equation of cumulative deformation of rock subjected to multiple disturbances and obtained the evolution law of the surrounding rock stress field caused by a blasting disturbance. Liu et al. [11] studied the effects of confining pressure on the mechanical properties and fatigue damage evolution of sandstone by using the MTS-815 rock test system. Tang et al. [12] carried out uniaxial small-amplitude high-stress cyclic disturbance tests on deep marble and established a strain damage model under cyclic loading. Based on the energy dissipation theory, Liu et al. [13] established a new damage model to describe the behavior of siltstone and sandy mudstone subjected to cyclic loading and calculated the damage evolution equation of siltstone and sandy mudstone. Liu et al. [14] carried out cyclic loading tests on marble, skarn, and serpentine under different stress amplitudes and

analyzed the evolution law of damage variables in response to these variations. Huang [15] studied the fatigue damage characteristics of gypsum under cyclic loading and established a creep damage constitutive model of gypsum. Sun et al. [16] analyzed the damage evolution law and accumulation mode of sandstone subjected to cyclic loading under different confining pressures. Liu et al. [17] studied the creep failure characteristics of soft rock under dynamic disturbance through a self-developed rock disturbance and creep experimental system and established a disturbance creep constitutive model of soft rock based on a disturbance factor. Zhao et al. [18] found that under short-term cyclic loading of sandstone, both the residual strain and peak strain show the "decay increase" and "steady-state increase" stages with the cyclic number N, and they used a modified Burgers model to establish the relationship between the strain and cyclic number N under peak stress (tensile or compressive stress). Wang et al. [19] carried out uniaxial disturbance creep tests of gneiss under different disturbance amplitudes and frequencies and obtained the influence of disturbance load on rock creep characteristics.

The above research results establish rock constitutive relationships and rock damage characteristics based on the energy and cyclic number or reveal the mechanical characteristics of disturbed rock from the angle of stress amplitude and frequency. The methods seldom use the cyclic number and frequency in the same constitutive equation in order to define the law of rock strain damage.

2. Test Equipment and Scheme

2.1. Test Equipment and Specimen Preparation. The mechanical properties of sandstone under cyclic loading are studied by using a TAW-2000 rock triaxial testing machine (see Figure 1). Firstly, the mechanical properties of sandstone under different stress amplitudes are studied by fixing loading frequency. Then, the mechanical properties of rock under different loading frequencies are studied by fixing the stress amplitude. During the test, the specimens are loaded axially to a certain value, σ_{max}, and then cyclically loaded in stages. The loading process is shown in Figure 2.

The sandstone samples are taken from the roadway roof with a buried depth of 800 m in the West Third mining area of Hongyang No. 2 Mine, Sujiatun District, Shenyang city, Liaoning Province, China. The samples are a fine sandstone with high hardness and homogeneity, with a porosity of 2.5%. In compliance with the test procedures listed by International Society of Rock Mechanics [20], the shape of all tested sandstone specimens is cylindrical with 50 mm in diameter and 100 mm in length, approximately. In order to ensure the consistency of physical and mechanical properties of the specimens, the specimens with rough, uneven, or defective surfaces are not used. The specimens are then tested for their propagation velocity in response to a P wave. Based on these results, the testing specimens with close propagation velocities of the P wave are selected. The specimens are divided into three groups. Before the test, the parameters such as the diameter, circumference, and weight

Figure 1: TAW-2000 rock triaxial testing machine.

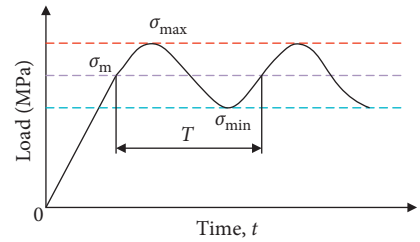

Figure 2: Cyclic disturbance loading.

of specimens are measured, and the density of each specimen is calculated. The grouping and physical parameters of the specimens are shown in Table 1.

2.2. Test Scheme. In order to study the mechanical response characteristics of sandstone under different stress amplitudes and loading frequencies, the test process is divided into three steps. The first group is used for uniaxial compression tests to obtain the uniaxial compressive strength of sandstone specimens in order to choose a reasonable upper limit σ_{max} and lower limit value σ_{min}. Then, the second group is used for fatigue damage tests under different cyclic stress amplitudes at a frequency of 0.5 Hz. The third group is used for fatigue damage tests under different loading frequencies at a stress amplitude of 5 MPa.

The stress-velocity control method is adopted in the test. The specimen is loaded to the upper limit of cyclic loading at a speed of 0.5 MPa/s under axial compression, and then the cyclic test is carried out with 1000 cycles per stage.

3. Test Results and Analysis

The uniaxial compressive strength R_c, yield strength σ_0, elastic modulus E, and Poisson's ratio μ of sandstone are obtained from averaging the results from the uniaxial compressive tests, as shown in Table 2.

3.1. Influence of Stress Amplitude on Fatigue Characteristics. Disturbance load is transmitted as a wave in the specimen. Disturbance waves can cause damage and deformation of rock and can be divided into two main cases. One is that disturbance waves propagate as elastic waves, in which there will be no permanent deformation nor crack propagation.

Table 1: Parameters for different specimens tested.

Groups	Specimen	D (mm)	L (mm)	M (g)	ρ (g·cm^{-3})	Average density (g·cm^{-3})	Loading mode	σ_{max} (MPa)	σ_{min} (MPa)	f (Hz)	Failure strength (MPa)	Cycle number
1	U1	50.10	99.84	520.3	2.645	2.630	Uniaxial compression	—	—	—	65.6	—
	U2	49.42	100.02	502.1	2.618		Uniaxial compression	—	—	—	67.5	—
	U3	48.82	99.78	490.4	2.627		Uniaxial compression	—	—	—	68.0	—
2	C-A1	48.84	98.64	483.4	2.617	2.620	Cyclic loading	35	25	0.5	—	1000
	C-A2	49.10	99.43	496.6	2.639		Cyclic loading	45	25	0.5	—	1000
	C-A3	48.30	100.20	478.4	2.607		Cyclic loading	55	25	0.5	55	297
3	C–F1	49.02	100.3	499.8	2.642	2.630	Cyclic loading	45	40	0.5	—	1000
	C–F2	48.24	99.90	474.9	2.602		Cyclic loading	45	40	1	—	1000
	C–F3	48.44	100.2	487.2	2.640		Cyclic loading	45	40	2	—	1000

Table 2: Static parameters of sandstone.

R_c (MPa)	σ_0 (MPa)	E (GPa)	μ
67	50	5	0.18

The other is disturbance propagation in the form of plastic waves. In this case, the original cracks propagate and penetrate, creating new cracks. The plastic deformation accumulates gradually, and the specimen eventually fails.

In Figure 3, it can be seen that when the upper limit stress (peak stress) is 35 or 45 MPa, no fatigue damage occurs in the specimens after 1000 cycles. When peak stress is 55 MPa, the specimen fails after 297 cycles, which verifies that there is an upper limit threshold in cyclic loading. If the peak stress is lower than this value, no matter how many cycles are loaded, the specimen will not be destroyed. The critical stress lies between 45 and 55 MPa in which plastic deformation and failure will result. If the peak stress is higher than 55 MPa, the specimen will be destroyed in 1000 cycles or less. This shows that the fatigue life of sandstone is reduced with peak stresses greater than 55 MPa and is unaffected by peak stresses less than 45 MPa. Further testing is required in order to find the critical peak failure stress in cyclic loading within the range of 45 to 55 MPa.

The stress-strain hysteresis curves of the specimens under cyclic loading are cusp-shaped, rather than oval-shaped, at the place of stress inversion, which indicates that the elastic deformation response of the specimens is faster than the plastic deformation response. As the stress amplitude increases, the hysteretic curve moves to the right gradually, the hysteretic loop area increases gradually, the transverse spacing of a single hysteretic loop widens, and the axial strain increases. This trajectory indicates the damage accumulated and energy dissipated with the repeated opening and closing of a microfracture. The energy loss and irreversible deformation caused by the damage increase with an increase in stress amplitude.

Figure 4 shows the relationship between the axial peak strain and the cycle number N. Under cyclic loading between 25 and 35 MPa, the axial peak strain increases gradually and then reaches a relative stability value of about 0.77%, and it is

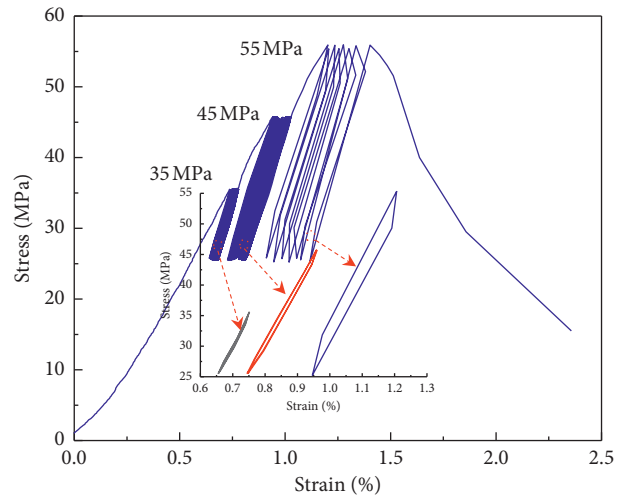

Figure 3: Stress-strain curves under different stress amplitudes.

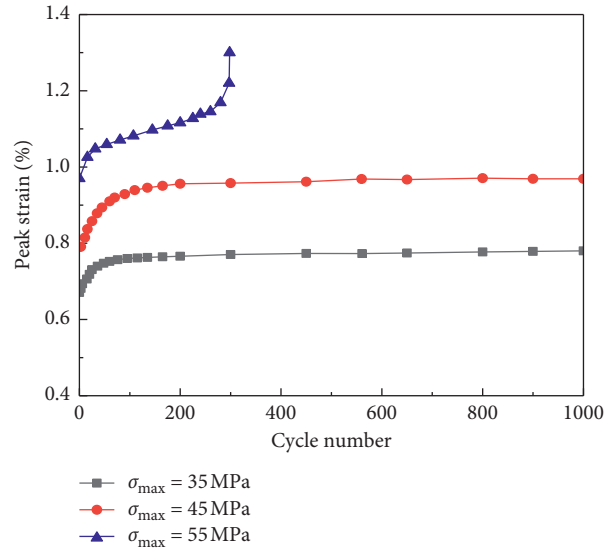

Figure 4: Peak strain evolution curve.

still 0.77% for the remaining cycles. For the cyclic loading between 25 and 45 MPa, the axial peak strain increases gradually and then reaches a stable value of 0.95%, following which it remains unchanged. When cycling between 25 and 55 MPa, the axial strain continues to increase with cycle number and does not reach a stable value. The fatigue damage of sandstone under cyclic loading between 25 and 55 MPa undergoes three stages: the first stage is the initial stage, in which the strain rate decreases gradually; the second stage is the stable stage, in which the strain rate remains relatively unchanged; and the third stage is the accelerated stage, in which the strain rate increases rapidly.

3.2. Effect of Loading Frequency on Fatigue Characteristics of Sandstone. Figure 5 shows the stress-strain curves of the specimens at frequencies of 0.5 Hz, 1 Hz, and 2 Hz under a stress amplitude of 5 MPa. As loading frequency increases, the hysteresis loops become denser, which indicates that the growth rate of plastic deformation is decreasing gradually. After the 2 Hz cycling, the specimens are not damaged and are in a fatigue stability stage, but irreversible plastic deformation occurs after unloading.

As can be seen from Figure 6, as frequency increases, the strain remains unchanged, which is different from previous research that showed strain of salt rock and gypsum rock decreasing with increasing frequency [9, 15]. Hence, during cyclic loading, the specimen enters the plastic deformation stage and remains in a stable fatigue stage with increasing loading frequency. However, to monitor the variation of internal cracks in rocks, it is necessary to further observe internal cracks through electron microscopy or CT.

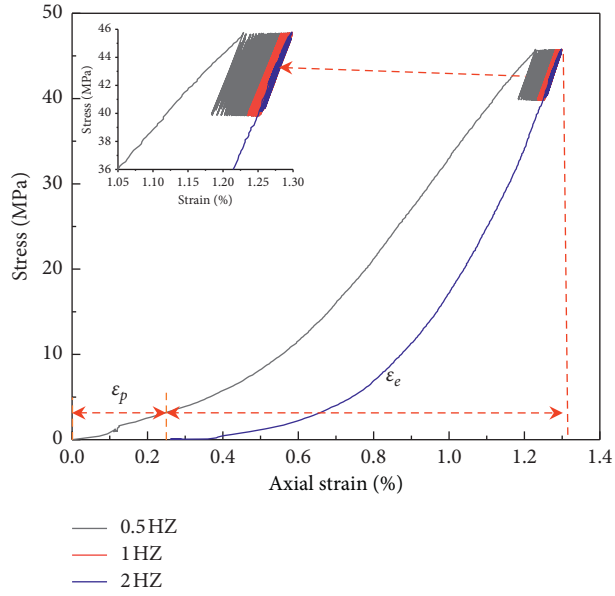

Figure 5: Stress-strain curves under different loading frequencies.

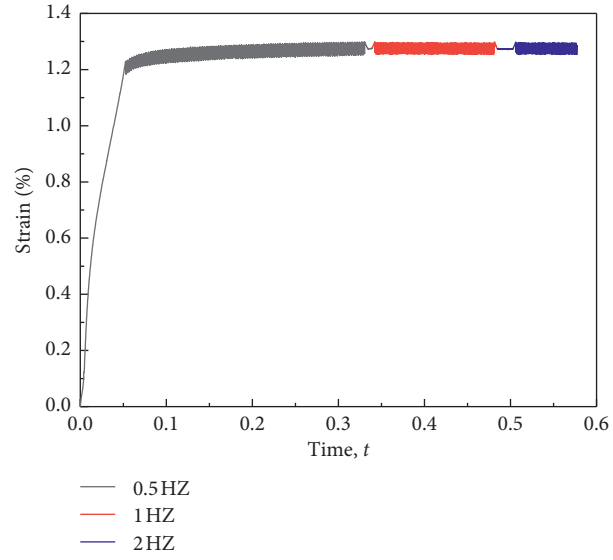

Figure 6: Strain-time curves under different loading frequencies.

4. Establishment of Sandstone Damage Constitutive Model under Disturbance

4.1. Model Selection. When rocks are subjected to repeated disturbance loads, internal structural distortion and crack evolution lead to cumulative damage and irreversible plastic deformation. At present, the description of damage evolution is mainly based on the evolution characteristics of damage variable D. Kachanov [21] established the relationship between the creep damage variable and creep time of brittle rock.

$$D = 1 - \left(1 - \frac{t}{t_R}\right)^{(1/r+1)}, \quad (1)$$

where t_R is the creep life and r is the parameter of rock material properties.

In a cyclic loading test, the rock fatigue life N_f is the number of cycles at the time of rock failure. If T is the time for one cycle, then the cycle number and loading time satisfy $t = NT$ and $t_R = N_f T$, and then (1) can be expressed as

$$D = 1 - \left(1 - \frac{N}{N_f}\right)^{(1/r+1)}. \quad (2)$$

It can be seen that this expression for damage under cyclic loading is similar to that of creep damage, and the essence of damage variable is the same. For both cases, under the action of external load over a given cycle number or time frame, rock material properties will deteriorate due to internal structure distortion, crack initiation and propagation, and continuous energy dissipation. It can be seen from Figure 4 that the peak strain curve under cyclic loading has the same evolution law as that under creep loading, which also follows the three-stage characteristics listed in Section 3.1. Based on the above two points, it is considered that the damage failure of specimens subjected to cyclic loading is essentially the rock creep under peak stress. Therefore, this paper will study the damage characteristics of sandstone under cyclic loading based on creep theory.

In view of the disturbance of geotechnical materials under external loads, Desai, an American scholar, proposed

the concept of disturbed state concept (DSC) [22]. The DSC holds that material structure is composed of an undisturbed relative-integrity state (RI state) and completely destroyed fully adjusted state (FA state). The material structure can transform from RI state to FA state under external force. The function describing the transformation process between these two states is called the disturbed function (D). The expression of their relationship is

$$\varepsilon_{ij} = (1 - D)\varepsilon_{ij}^{i} + D\varepsilon_{ij}^{c}, \tag{3}$$

where ε_{ij}, ε_{ij}^{i}, and ε_{ij}^{c} are observed strain values, RI strain values, and FA strain values, respectively.

Based on creep theory and the disturbance state concept, the strain damage model of sandstone under different peak stresses is established in this paper. According to the strain curves of sandstone under different peak stresses, the specimen exhibits elastic deformation at the moment of loading. As the cycle number increases, the specimen continues to deform, and the deformation rate gradually decreases, showing viscous characteristics. Then, irreversible plastic deformation occurs, ultimately rupturing the rock specimen. Therefore, the selected model should contain the elastic, viscous, and plastic elements in order to reflect the complete process of strain damage evolution.

(a) Sandstone in an RI state is considered to have viscoelastic deformation under external disturbance. In order to simplify the model and reduce the parameters, the Kelvin model is used to represent sandstone in RI state. The equation is as follows:

$$\varepsilon = \frac{\sigma}{E_1}\left(1 - e^{\left(-\left(E_1/\eta_1\right)t\right)}\right), \tag{4}$$

where E_1 and η_1 are elastic fatigue coefficient and viscous coefficient of the Kelvin body, respectively.

(b) After entering FA state, the material in RI state encloses and restricts the material in FA state during deformation, which locally hardens the material in FA state. However, after continuous disturbance, the specimen eventually breaks down, so it can be represented by a model with a critical state. Huang [15] considered that the sudden change of fatigue rate will be triggered if the disturbance force exceeds a certain critical value. A nonlinear disturbance creep element (NDCE) is introduced (see Figure 7).

The nonlinear disturbance creep element satisfies

$$\sigma - \sigma_s = \frac{\eta_3}{t^{n-1}} \cdot \left(\frac{d\varepsilon}{dt}\right)^m, \quad \sigma > \sigma_s, \tag{5}$$

where η_3 is viscous coefficient of the nonlinear clay body, n is rheological coefficient, t is rheological time, m is the parameter of rock property ($0 \le m \le 1$), and σ_s is threshold stress, which is considered as yield strength.

When $\varepsilon\ (0) = 0$, (5) can be transformed using the separation of variables method such that

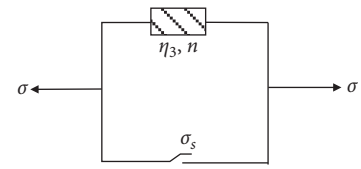

Figure 7: Nonlinear disturbance creep element.

$$\varepsilon(t) = \left(\frac{\sigma - \sigma_s}{\eta_3}\right)^{(1/m)} \frac{m}{m + n - 1} t^{(m+n-1/m)}, \quad \sigma > \sigma_s. \tag{6}$$

The FA state model is obtained by connecting the NDCE in series with the traditional Maxwell creep model (see Figure 8).

The state equation of the improved Maxwell model:

$$\begin{cases} \sigma_1 = E_2\varepsilon_1, \\ \sigma_2 = \eta_2\dot{\varepsilon}_2, \\ \sigma_3 = \sigma_s + \dfrac{\eta_3}{t^{n-1}} \cdot \left(\dfrac{d\varepsilon}{dt}\right)^m, \\ \sigma = \sigma_1 = \sigma_2 = \sigma_3, \\ \varepsilon = \varepsilon_1 + \varepsilon_2 + \varepsilon_3. \end{cases} \tag{7}$$

Combining (6) and (7), we obtain the disturbance model.

$$\varepsilon = \begin{cases} \dfrac{\sigma}{E_2} + \dfrac{\sigma}{\eta_2}t, & (\sigma > \sigma_s), \\ \dfrac{\sigma}{E_2} + \dfrac{\sigma}{\eta_2}t + \left(\dfrac{\sigma_1 - \sigma_s}{\eta_3}\right)^{(1/m)} \dfrac{m}{m + n - 1} t^{(m+n-1/m)}, & (\sigma > \sigma_s), \end{cases} \tag{8}$$

where E_2 and η_2 are elastic fatigue coefficient and viscous coefficient of the Maxwell body, respectively.

(c) According to Guo [23], the disturbance function D is a function with plastic cumulative strain value ε^p as an independent variable. Assuming that the disturbance function D is in the form of a Weibull function, we obtain

$$D = D\left(\varepsilon^p\right) = D_u\left\{1 - \exp\left[\left(-\alpha\varepsilon^p\right)^\beta\right]\right\}, \tag{9}$$

where α and β are the scale and shape parameters of rocks; D_u is the disturbance limit, $0 \le D_u \le 1$, and $D_u = 1$ generally; and ε^p is the plastic cumulative strain value.

The total strain can be divided into two parts: elastic strain and plastic strain. According to the Manson–Coffin empirical formula [24, 25], the total strain is expressed using the cycle number and loading frequency as

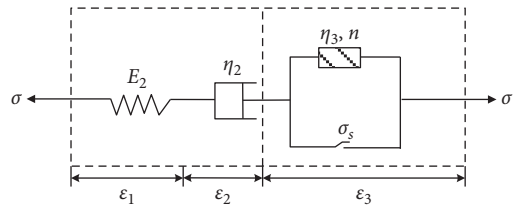

Figure 8: Improved Maxwell model.

$$\varepsilon = \varepsilon^e + \varepsilon^p = c_1\left(Nf^{k_1-1}\right)^{-\beta_1} + c_2\left(Nf^{k_2-1}\right)^{-\beta_2}, \quad (10)$$

where f is loading frequency; c_1, c_2, k_1, k_2, β_1, and β_2 are material constants; ε^e and ε^p are the elastic strain and plastic strain, respectively; and N is cycle number.

Hence, the relationship between loading frequency and plastic strain ε^p is as follows:

$$\varepsilon^p = c_2\left(Nf^{k_2-1}\right)^{-\beta_2}. \quad (11)$$

(d) The cycle number and loading time satisfy $t = N\mathrm{T}$. Combining Equations (3), (4), (8), (9), and (11), we can obtain the expression of one-dimensional sandstone strain damage:

$$\varepsilon(N) = \begin{cases} \left[1 - e^{-\left(AN^{-B}f^{C}\right)}\right] \cdot \left[\dfrac{\sigma}{E_1}\left(1 - e^{-\left((E_1/\eta_1)N\mathrm{T}\right)}\right)\right] + e^{-\left(AN^{-B}f^{C}\right)} \cdot \left[\dfrac{\sigma}{E_2} + \dfrac{\sigma}{\eta_2}N\mathrm{T}\right], & (\sigma < \sigma_s), \\ \left[1 - e^{-\left(AN^{-B}f^{C}\right)}\right] \cdot \left[\dfrac{\sigma}{E_1}\left(1 - e^{-\left((E_1/\eta_1)N\mathrm{T}\right)}\right)\right] + e^{-\left(AN^{-B}f^{C}\right)} \cdot \left[\dfrac{\sigma}{E_2} + \dfrac{\sigma}{\eta_2}N\mathrm{T} + \left(\dfrac{\sigma - \sigma_s}{\eta_3}\right)^{(1/m)}\dfrac{(N\mathrm{T})^G}{G}\right], & (\sigma > \sigma_s), \end{cases}$$

$$A = (\alpha \cdot c_2)^{\beta},$$

$$B = \beta \cdot \beta_2,$$

$$C = (1 - k_2) \cdot \beta \cdot \beta_2,$$

$$G = \left(\frac{m + n - 1}{m}\right), \quad (12)$$

where σ is stress; ε is strain; N is cycle number; f is loading frequency; T is loading period, $T = 1/f$; σ_s is threshold stress, which is considered as yield strength; E_1 and E_2 are elastic fatigue coefficients of the Kelvin body and Maxwell body, respectively; η_1 and η_2 are viscous coefficients of the Kelvin body and Maxwell body, respectively; η_3 is viscous coefficient of the nonlinear clay body; and A, B, C, G are material constants related to c_1, c_2, k_1, k_2, β_1, and β_2.

The modified strain damage model of sandstone is shown in Figure 9.

4.2. Parameter Identification of Model. According to the peak strain of sandstone under uniaxial cyclic loading, the strain damage equation is fitted using Origin software and the least squares principle, and the parameters of the strain damage model are obtained as shown in Table 3. When cycling to a peak stress of 55 MPa, both E_2 and η_2 in the Maxwell body increase significantly, which may be due to the hardening of the specimen before failure.

The strain damage model of sandstone based on the concept of a disturbance state is compared with the experimental results as shown in Figure 10. The experimental results under different stress amplitudes are represented by symbols of different shapes, and the theoretical calculated values are expressed by solid lines. The derived constitutive model is in good agreement with the experimental results and reflects the characteristic three stages of sandstone damage failure under cyclic loading, which verifies the presented strain damage model of sandstone based on disturbance state.

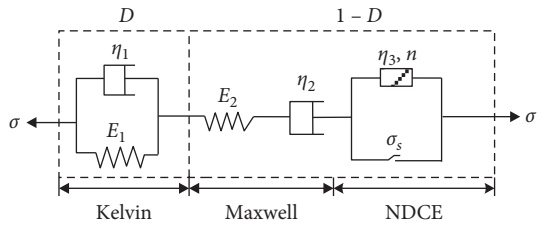

Figure 9: Strain damage model of sandstone.

Table 3: Strain damage model parameters of sandstone under disturbance state concept.

σ_{max} (MPa)	Model parameter										Fitting effect
	A	B	C	E_1 (MPa)	E_2 (MPa)	η_1 (MPa·N)	η_2 (MPa·N)	η_3 (MPa·N)	n	m	R^2
35	0.74	0.36	0.31	45.10	52.17	6.42	61998.51				0.992
45	0.09	0.69	0.60	46.39	56.95	3.82	70311.99				0.991
55	84.00	0.04	9.46	12.55	21930.55	2.28	286624.7	5.10	8.9	0.57	0.962

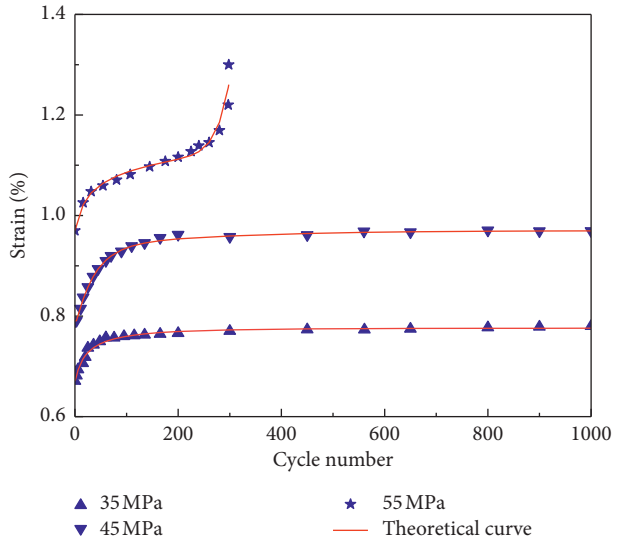

Figure 10: Comparison of strain damage model values with test curves.

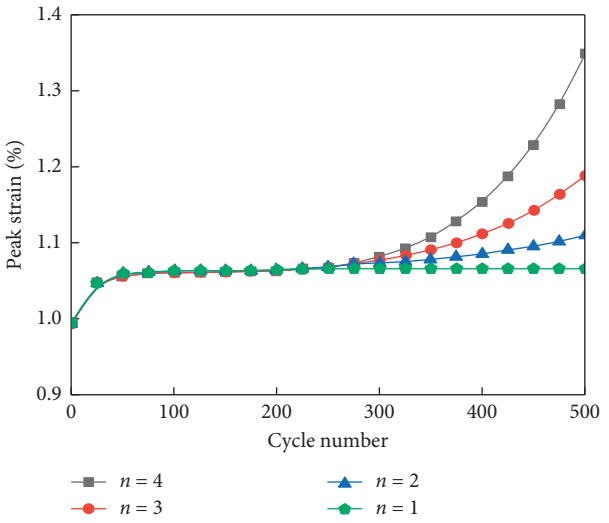

Figure 11: Influence of rheological parameter n on the mode.

Figure 11 shows the variation of the strain damage curve with rheological coefficient n when the peak stress is fixed at 55 MPa. The acceleration phenomenon becomes more and more obvious as coefficient n increases. The change of n mainly affects the accelerated failure stage and has no measurable effect on the first and second stages of strain evolution. This shows that the nonlinear clay body can simulate the accelerated damage stage of sandstone well and verify the rationality of the model.

Figure 12 shows the variation curve of disturbance function D with the cycle number under different peak stresses. When the peak stress is 35 or 45 MPa, the slope of the curve increases gradually, with 35 MPa showing a sharper initial slope increase in early cycles. While cycling up to 1000 cycles, the disturbance function value tends to be stable and less than 1 for both cases, which indicates that the specimens were not damaged. This is similar to the variation rule of the peak strain curve. When peak stress increases to

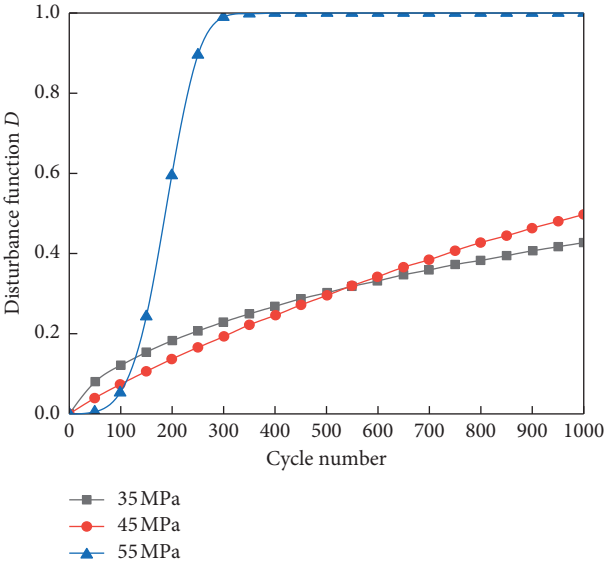

Figure 12: Change curve of disturbance function.

55 MPa, the second derivate of the slope is initially positive before inverting around 150 cycles. For this case, D continues to sharply increase until reaching a value of 1 at 297 cycles when the rupture of the rock specimen takes place. The 55 MPa peak stress cycling process reflects the transformation from RI state to FA state, controlled by the disturbance function.

5. Conclusion

(1) There exists an upper threshold value for the axial stress of sandstone under cyclic loading. When the loading frequency is constant, with the increase of stress amplitude, the area of hysteresis loop increases gradually, the transverse spacing of a single hysteresis curve widens, and the energy loss and irreversible deformation of rock caused by damage increase gradually. When the stress amplitude is constant (mean stress value of 42.5 MPa and amplitude of 5 MPa), an increase in loading frequency did not change the axial strain.

(2) The unstable fatigue damage of sandstone subjected to cyclic loading generally goes through three stages: the initial stage in which the strain rate decreases gradually, the stable stage in which the strain rate remains unchanged, and the accelerated failure stage in which the strain rate increases rapidly.

(3) On the basis of creep theory and the disturbance state concept, a strain damage model of sandstone is established. The parameters of the model are solved by Origin software. The rationality and correctness of the strain damage model are validated by comparing the calculated results with the experimental data.

Data Availability

The test data used to support the findings of this study are available from the corresponding author upon request.

Conflicts of Interest

The authors declare that they have no conflicts of interest.

Acknowledgments

This study was supported by the National Key R&D Program of China (grant no. 2018YFC0604705), National Natural Science Foundation of China (grant no. 51774167), and Science and Technology Innovation Leading Talent Project of Liaoning Province (grant no. XLYC1802063).

References

[1] A. Taheri, A. Royle, Z. Yang, and Y. Zhou, "Study on variations of peak strength of a sandstone during cyclic loading," *Geomechanics and Geophysics for Geo-Energy and Geo-Resources*, vol. 2, pp. 1–10, 2016.

[2] G.-L. Feng, X.-T. Feng, B.-R. Chen, and Y.-X. Xiao, "Microseismic sequences associated with rockbursts in the tunnels of the Jinping II hydropower station," *International Journal of Rock Mechanics and Mining Sciences*, vol. 80, pp. 89–100, 2015.

[3] A. Momeni, M. Karakus, G. R. Khanlari, and M. Heidari, "Effects of cyclic loading on the mechanical properties of a granite," *International Journal of Rock Mechanics and Mining Sciences*, vol. 77, pp. 89–96, 2015.

[4] X. Li, Z. Zhou, T.-S. Lok, L. Hong, and T. Yin, "Innovative testing technique of rock subjected to coupled static and dynamic loads," *International Journal of Rock Mechanics and Mining Sciences*, vol. 45, no. 5, pp. 739–748, 2008.

[5] F. J. Zhao, X. B. Li, and T. Feng, "Research on experiments of brittle rock fragmentation by combined dynamic and static loads," *Rock and Soil Mechanics*, vol. 2005, no. 7, pp. 1038–1042, 2005.

[6] Y. J. Zuo, X. B. Li, C. A. Tang, Y. P. Zhang, C. D. Ma, and C. B. Yan, "Experimental investigation on failure of rock subjected to 2D dynamic-static coupling loading," *Chinese Journal of Rock Mechanics and Engineering*, vol. 2006, no. 9, pp. 1809–1820, 2006.

[7] Y.-j. Zuo, X.-b. Li, Z.-l. Zhou, C.-d. Ma, Y.-p. Zhang, and W.-h. Wang, "Damage and failure rule of rock undergoing uniaxial compressive load and dynamic load," *Journal of Central South University of Technology*, vol. 12, no. 6, pp. 742–748, 2005.

[8] R. Song, B. Yue-ming, Z. Jing-Peng, J. De-yi, and Y. Chun-he, "Experimental investigation of the fatigue properties of salt rock," *International Journal of Rock Mechanics and Mining Sciences*, vol. 64, pp. 68–72, 2013.

[9] J. Y. Fan, *Fatigue damage and dilatancy properties for salt rock under discontinuous cyclic loading*, PhD thesis, Chongqing University, Chongqing, China, 2017.

[10] B. Wang, Y. F. Gao, and J. Wang, "Evolution law analysis on surrounding rock stress field by rheology disturbed effects," *Journal of China Coal Society*, vol. 35, no. 9, pp. 1446–1450, 2010.

[11] E. Liu and S. He, "Effects of cyclic dynamic loading on the mechanical properties of intact rock samples under confining pressure conditions," *Engineering Geology*, vol. 125, pp. 81–91, 2012.

[12] L. Z. Tang, J. L. Wu, T. Liu, J. Zhu, and J. B. Shu, "Mechanical experiments of marble under high stress and cyclic dynamic disturbance of small amplitude," *Journal Of Central South University (Science And Technology)*, vol. 45, no. 12, pp. 4300–4307, 2014.

[13] X. S. Liu, J. G. Ning, Y. L. Tan, and Q. H. Gu, "Damage constitutive model based on energy dissipation for intact rock subjected to cyclic loading," *International Journal of Rock Mechanics and Mining Sciences*, vol. 85, pp. 27–32, 2016.

[14] T. Liu, P. Yang, W. S. Lv, and K. Du, "Rock mechanical properties experiments with low-frequency circulation disturbance under different stress amplitudes," *Journal of China Coal Society*, vol. 42, no. 9, pp. 2280–2286, 2017.

[15] X. Huang, "Fatigue damage characteristics and constitutive model of gypsum rock under cyclic loading," Master thesis, Chang'an University, Xi'an, China, 2017.

[16] B. Sun, Z. Zhu, C. Shi, and Z. Luo, "Dynamic mechanical behavior and fatigue damage evolution of sandstone under cyclic loading," *International Journal of Rock Mechanics and Mining Sciences*, vol. 94, pp. 82–89, 2017.

[17] F. Liu, Y. J. Yu, L. Z. Cao, W. Zhang, and G. N. Zhang, "Constitutive model of soft rock disturbance creep based on disturbance factor," *Journal of China Coal Society*, vol. 43, no. 10, pp. 2758–2764, 2018.

[18] B. Y. Zhao, D. Y. Liu, and W. Liu, "Mechanical behavior of sandstone under uniaxial constant cyclical compressive and tensile loading," *Arabian Journal of Geosciences*, vol. 11, no. 17, p. 490, 2018.

[19] J. G. Wang, B. Liang, and P. J. Yang, "Creep experiment and nonlinear disturbance creep model of gneiss under dynamic and static loads," *Journal of China Coal Society*, vol. 44, no. 1, pp. 192–198, 2019.

[20] ISRM, "Suggested methods for determining the strength of rock material in triaxial compression," *International Journal of Rock Mechanics and Mining Sciences and Geomechanics Abstracts*, vol. 15, no. 2, pp. 47–51, 1978.

[21] M. Kachanov, "Effective elastic properties of cracked solids: critical review of some basic concepts," *Applied Mechanics Reviews*, vol. 45, no. 8, pp. 304–335, 1992.

[22] C. S. Desai and A. Gens, "Mechanics of materials and interfaces: the disturbed state concept," *Journal of Electronic Packaging*, vol. 123, no. 4, p. 406, 2001.

[23] Z. K. Guo, "Study on models and solution of fem basic formulation of theory of duality disturbance," Master thesis, Shenyang Jianzhu University, Shengyang, China, 2011.

[24] L. F. Coffin, "The effect of frequency on the cyclic strain and low cycle fatigue behavior of cast Udimet 500 at elevated temperature," *Metallurgical and Materials Transactions B*, vol. 2, no. 11, pp. 3105–3113, 1971.

[25] Y. Wang, L. Ma, P. Fan, and Y. Chen, "A fatigue damage model for rock salt considering the effects of loading frequency and amplitude," *International Journal of Mining Science and Technology*, vol. 26, no. 5, pp. 955–958, 2016.